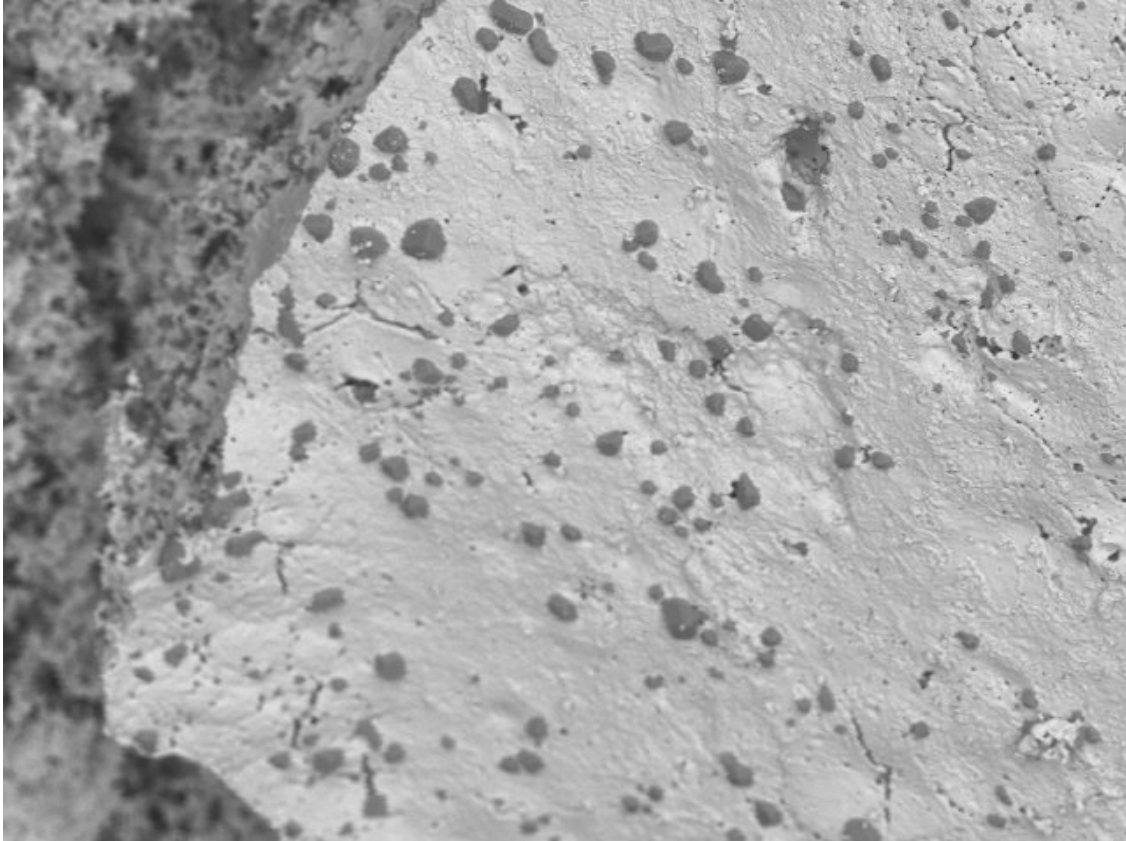




CHALMERS
UNIVERSITY OF TECHNOLOGY



Stabilization of Uranium Nitride by Aluminum and Chromium Doping

Master's thesis in Master Programme Materials Chemistry

Einar Axhage

DEPARTMENT OF CHEMISTRY AND CHEMICAL ENGINEERING
CHALMERS UNIVERSITY OF TECHNOLOGY
Gothenburg, Sweden 2022
www.chalmers.se

MASTER'S THESIS 2022

EINAR AXHAGE



CHALMERS
UNIVERSITY OF TECHNOLOGY

Department of Chemistry and Chemical Engineering
Division of Energy and Materials
Nuclear Chemistry and Industrial Materials Recycling
CHALMERS UNIVERSITY OF TECHNOLOGY
Gothenburg, Sweden 2022

© EINAR AXHAGE, 2022.

Supervisor: PhD Cand. Luis G.Gonzales F.
Nuclear Chemistry and Industrial Materials Recycling

Supervisor: Prof. Teodora Retegan Vollmer
Nuclear Chemistry and Industrial Materials Recycling

Examiner: Prof. Christian Ekberg
Nuclear Chemistry and Industrial Materials Recycling

Master's Thesis 2022
Department of Chemistry and Chemical Engineering
Division of Energy and Materials
Nuclear Chemistry and Industrial Materials Recycling

Chalmers University of Technology
SE-412 96 Gothenburg
Telephone +46 31 772 1000

Cover: SEM image of a chromium doped uranium nitride microsphere with darker formations caused by the limited solubility of chromium in the uranium nitride phase.

Typeset in L^AT_EX
Printed by Chalmers Reproservice
Gothenburg, Sweden 2022

EINAR AXHAGE

Department of Chemistry and Chemical Engineering
Chalmers University of Technology

Abstract

Uranium nitride is a promising accident tolerant fuel (ATF) candidate as it has great uranium density and thermal conductivity. The main downside is its inherent weakness to oxidation in mainly water and steam. In this work, uranium nitride was synthesized with 20% of total molar metal content as varying amounts of aluminum and chromium. The material was investigated in terms of oxidation performance and microstructure in order to assess the suitability of said dopants as an approach of stabilization. The material was synthesized as microspheres via the internal sol-gel process and carbothermal reduction at 1550 °C.

Aluminum caused a change in microstructure and made the material more porous, which was believed to be the main reason why aluminum reduced oxidation performance during thermogravimetric analysis. This change was attributed to the tendency of aluminum to collect along the grain boundaries, potentially weakening grain adhesion. Only when chromium alone was added the oxidation temperature was increased. Added chromium not only caused cracking due to the release of gasses, but also surface formations due to the limited solubility of chromium in uranium nitride.

Keywords: LWR, UN, ATF, sol gel, chromium, aluminum, doping, microsphere

Acknowledgements

I thank the people at the division of Energy and Materials for letting me participate in this research project and assisting me in my work. I greatly value the knowledge and experience I've gain throughout both my bachelor's and master's thesis projects in the field of nuclear chemistry.

Einar Axhage, Gothenburg, June 2022

This research was financially supported by the Swedish Foundation for Strategic Research (SSF), project number EM16-0031.

List of Acronyms and Chemical Formulae

Below is the list of repeated acronyms and chemical formulae that have been used throughout this thesis listed in alphabetical order:

AlN	Aluminum nitride
ATF	Accident Tolerant Fuel
Al ₂ O ₃	Alumina
Cr ₂ O ₃	Chromia
CrN	Chromium nitride
EDX	Energy Dispersive X-ray
HMTA	Hexamethylenetetramine
ICP-MS	Inductively Coupled Plasma Mass Spectrometry
IGP	Internal Gelation Process
LWR	Light Water Reactor
PWR	Pressurized Water Reactor
SEM	Scanning Electron Microscopy
TGA	ThermoGravimetric Analysis
TOC	Total Organic Carbon
TRISO	Tri-structural ISotropic particle fuel
UO ₂	Uranium (di)oxide
UN	Uranium nitride
U ₃ Si ₂	Uranium silicide
XRD	X-Ray Diffraction

Contents

List of Acronyms and Chemical Formulae	ix
1 Introduction	1
1.1 Background	2
1.1.1 Fundamentals of Nuclear Energy and Fuel	2
1.1.2 Nuclear Reactor Types	2
1.1.3 Fuel Assembly and Cladding	3
1.1.4 ATF Candidates	4
1.1.5 UN Fuel	5
1.1.6 UN Dopants	7
1.2 Aim and Limitations	8
2 Theory	9
2.1 Internal Sol-Gel Process	9
2.2 Reduction to UO_2	10
2.3 Carbothermal Reduction to UN	10
2.4 Oxidation and Hydrolysis of UN	11
2.5 Chemistry of Dopant Metals	12
3 Method	13
3.1 Batch Profiles and Indexing	13
3.2 Production of Gel-Microspheres	14
3.3 Reduction and Nitridation	15
3.4 Analytical Instruments and Procedure	17
3.4.1 SEM/EDX	17
3.4.2 XRD	17
3.4.3 ICP-MS	17
3.4.4 Carbon, Oxygen and Nitrogen Analysis	18
3.4.5 TGA	18
3.5 Chemicals	18

4	Results and Discussion	19
4.1	Synthesis, Microstructure and Elemental Distribution	19
4.2	Carbon, Oxygen and Nitrogen Analysis	23
4.3	XRD	24
4.4	ICP-MS	26
4.5	TGA	27
5	Conclusion	29
6	Future Work	31
	Bibliography	33

1

Introduction

After the nuclear accident at the Fukushima Daiichi power plant in Japan (2011), an increased international effort has been made to develop so called accident tolerant fuels (ATF) for the purpose of achieving improved fuel performance during accident conditions. In loss-of-coolant accidents seen in Fukushima and Three Mile Island (1979) where light water reactors (LWRs) were used, hydrogen gas was produced from water reacting with the zirconium-based fuel cladding at elevated temperatures. To avoid this problem the cladding material could be changed to FeCrAl alloy which has been researched in recent years [1]. One of the main problems with this cladding concept is the increased neutron penalties compared to conventional cladding materials. To counteract this penalty the uranium density in the fuel must be higher (without further enrichment) so that the neutron economy is balanced [2].

Uranium Nitride (UN) is a potential ATF candidate as it has numerous benefits compared to conventional uranium oxide (UO_2) used today, the main ones being higher uranium density and superior thermal conductivity. Thus, UN can improve the fuel economy while also reducing the internal operating temperature significantly [3] [1]. The main downside of UN is its well known tendency to oxidize in both air, steam and water [4] [5]. This not only makes the production process more difficult as it has to be done in an oxygen free atmosphere, but also poses a risk of fuel degradation and hydrogen gas development inside the reactor core during operation, should water and steam leak into the fuel.

In order to combat oxidation, methods of improving the corrosion resistance of UN by incorporating various elements have been studied and proposed [2] [6] [7]. If a protective oxide layer can be formed, the corrosion of the fuel can be slowed down. Two of these elements known for producing protective oxide layers at higher temperatures are aluminum and chromium.

One way of producing UN fuel pellets is through the internal sol-gel process (IGP) where an aqueous solution is gelled into droplet sized spheres through hydrolysis which are then reduced into UO_2 and nitrated to UN. The spheres - called microspheres - can then be pressed and sintered into pellets. The IGP method has numerous benefits to the conventional powder-process that is normally used. For example, the interaction with radioactive powders is kept at a minimum [8].

1.1 Background

In this section, the fundamentals of conventional nuclear energy is explained before covering ATF concepts and properties of UN fuel. Lastly, chromium and aluminum dopants for corrosion protection are introduced.

1.1.1 Fundamentals of Nuclear Energy and Fuel

The fundamental principle of any nuclear reactor used for energy production is to produce large amounts of heat through the fission - i.e. splitting of fissile atoms - sustained in a nuclear chain reaction [9]. The main nuclide used for fission in these reactors is ^{235}U which is the only fissile nuclide found in nature in quantities above trace amounts [10]. Fuel can also be made from a mixture of both ^{235}U and ^{239}Pu which is called mixed oxide (MOX) fuel. ^{239}Pu is a fissile metal formed when ^{238}U undergoes neutron capture during reactor operation, which then can be reprocessed and added back into the fuel cycle [11]. Natural uranium only consist of 0.7% ^{235}U which is why the metal has to be enriched through isotopic separation in order to be usable in most reactors. This process is mostly done by using gas centrifuges that separate gaseous uranium compounds by mass. The small relative difference in mass between the natural uranium isotopes makes them difficult to separate and the overall process energy demanding and expensive. Enrichment account for roughly half of the cost of nuclear fuel and around 5% of the total electricity cost. The total energy requirement also increases exponentially with desired level of enrichment. As this enrichment process also can be used to produce weapon-grade material there have been multiple international efforts to keep the production capacity under control as a non-proliferation measure [12].

1.1.2 Nuclear Reactor Types

The most common type of nuclear reactor used for electricity production is the LWR which makes up around 80% of all reactors in operation globally as of 2012 [13]. A LWR uses natural water (light water) as both moderator and primary coolant. The core is cooled by transferring heat into the water which turns into steam. In a Boiling Water Reactor (BWR) the water is boiled directly in a main coolant loop and in a Pressurized Water Reactor (PWR) the heat is transferred into a second loop where the boiling occurs instead. The steam produced is used to generate electricity by driving a steam turbine and then condensed and recirculated into the system [9].

The function of a moderator is to moderate - i.e. reduce the energy of the neutrons produced during fission. This is important because the original high-energy neutrons (called fast neutrons) have a very low chance of successfully hitting another ^{235}U target in order to cause a fission event and continue the chain reaction. This is why LWRs are so called thermal reactors, because they operate in the thermal spectrum which is the domain of low energy neutrons (called thermal or slow neutrons) [13]. Heavy water is a superior moderator to natural water which allows some heavy water reactors (HWR) to run on less enriched fuel or even natural uranium like the Canadian-Deuterium-Uranium reactor (CANDU) [14]. However, heavy water is exceedingly more expensive compared to natural water as it is composed of the heavier hydrogen isotopes deuterium which are isolated through isotopic separation. Moderators can also be made from solid graphite like the Soviet-made RBMK reactor, and many other materials [13]. Nuclear reactors can also operate in the fast spectrum which allows them to run without using any neutron moderation. However, these reactors are uncommon and can be considered to be a technological step beyond conventional thermal reactors used today. Fast reactors have numerous benefits in terms of increased fuel efficiency and reduced waste production [15].

1.1.3 Fuel Assembly and Cladding

The most common fuel type used in LWRs is UO_2 in the form of cylindrical pellets with a diameter of around 1 cm. These pellets are loaded into cylindrical tubes which are mounted in fuel assemblies that are aligned vertically inside the reactor core. These tubes are called cladding and have two main functions: protect the ceramic fuel from water induced corrosion and keep radioactive fission products from escaping into the coolant water. The material used for the cladding is a zirconium based alloy. Zirconium does not only have good anti-corrosion properties, but also have a low neutron absorption which is crucial to sustain the nuclear chain reaction [12] [16]. However, at higher temperatures zirconium reacts with water (Reaction 1.1) to form hydrogen gas which can result in explosions as seen in the Fukushima Daiichi accident in 2011 [13]. During this accident, temperature reached around 2800 °C [17] which caused a significant release of hydrogen gas. Zirconium alloys used in cladding form zirconia (ZrO_2) layers that protects the bulk material from further corrosion. However, at around 1200 °C a phase transition occurs from tetragonal to monoclinic [18], which accelerates corrosion significantly. Additionally, above 400 °C hydrogen is absorbed into the zirconium alloy which causes embrittlement due to hydride formation [13].



1.1.4 ATF Candidates

ATFs must keep or improve the properties compared to conventional fuels in the following areas [20]:

- Oxidation: Heat development caused by oxidation of the cladding should be reduced as well as the oxidation kinetics.
- Hydrogen development: The rate of hydrogen production via the cladding during normal operation should be lower.
- Durability: The cladding should be more tolerant to fracture and thermal damage or melting.
- Retention of fission products: The fuel and cladding system should increase the retention of radioactive fission products.
- Conductivity and Reactivity: The fuel should have higher thermal conductivity which reduces the internal operating temperature, as well as lower reactivity with the cladding and a higher melting point.

Along these potential improvements in reactor safety another significant focus in the development is improved economics, for example higher uranium metal content per fuel load which reduces reactor downtime and lower levels of enrichment which reduces the fuel production cost. Some potential ATF candidates are mentioned below and UN fuels are introduced in the next section.

TRISO Tri-structural ISOtropic particle fuel (TRISO) as a fuel concept originates from the High Temperature Reactor (HTR) design that operates at a temperature between 750 - 950 °C and normally helium cooled. The fuel is made from small (~0.5 mm) UO₂ pellets surrounded by layers of carbon or silicon carbide. These pebbles can then be arranged in a preferred medium like graphite. The TRISO fuel system is known for its high resistances to high temperatures and excellent retention of fission products. For the application as an ATF fuel, the TRISO fuel concept has been modified to be used as fuel in PWRs. This concept is known as Fully Ceramic Microencapsulated (FCM) fuel and is very similar. The kernel is made from UO₂ or UN and is incorporated into a silicon carbide matrix instead of graphite. This concept has some promising properties but still shares a significant downside with the standard TRISO concept, namely the high enrichment required for operation at around 20%.

U-Mo Uranium-Molybdenum fuel uses a uranium and molybdenum (10%) alloy instead of ceramic UO_2 . This makes the uranium metal content $\sim 70\%$ higher and increases the thermal conductivity by a tenfold. The fuel also have around half the heat capacity but on the downside also a lower melting point. The fuel design is annular (hollow) which improves the containment of fission products and allows the alloy to swell during operation. The surface of the alloy is enriched with a layer of aluminum, chromium and/or niobium which protects the alloy from water induced corrosion [21].

U_3Si_2 Uranium Silicide (U_3Si_2) fuel just like U-Mo fuel has a much higher thermal conductivity and metal density compared to UO_2 . Additionally, U_3Si_2 is also inherently resistant to water corrosion and has a much lower neutron absorption resulting in a better fuel economy. Similarly to other fuels types U_3Si_2 also swells as it accumulates fission products. It may be necessary to modify the material to reduce swelling before implementing it into reactor designs. This modification might result in a lower total uranium content compared to UO_2 [21].

1.1.5 UN Fuel

When looking at material properties for potential ATF candidates, UN show several promising characteristics (Table 1.1). The theoretical density is 30% higher than UO_2 which has obvious benefits in terms of total fissible material content in a reactor fuel assembly. It also improves the neutron economy which means that the fuel can operate at lower levels of enrichment or be used in environments with less optimal neutron moderation [1]. The thermal conductivity of UN is far superior and increases with temperature unlike UO_2 which has a negative thermal conductivity relationship with temperature (Figure 1.1). This results in a significantly lower operating temperature for UN compared to UO_2 . UN also has a lower thermal expansion coefficient which combined with the lower operating temperature results in less migration of fission products within the fuel.

Table 1.1: Comparison of material properties between UO_2 and UN [1]

Material Property	UO_2	UN
Heavy Metal Theoretical Density ($\text{kg} \cdot \text{m}^{-3}$)	1096	1430
Therm. cond. at 1100 °C ($\text{W} \cdot \text{m}^{-1} \cdot \text{K}^{-1}$)	2.8	22.8
Melting Point (°C)	2840	2762
Thermal Expansion Coefficient (10^{-6}K^{-1})	10	8

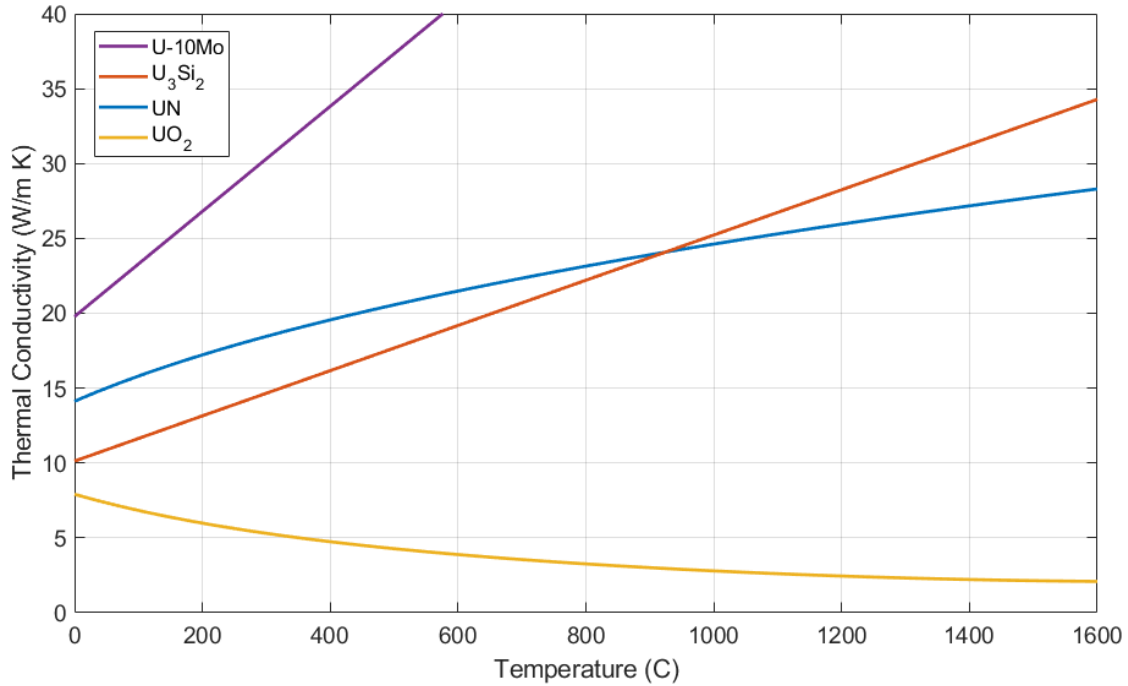


Figure 1.1: Thermal conductivity as a function of temperature for U-10Mo [23], U₃Si₂ [25], UN [24] and UO₂ [26].

Another downside of UN fuel apart from the oxidation issue is the parasitic neutron capture of ¹⁴N resulting in radioactive ¹⁴C through transmutation (Reaction 1.2) [20]. This parasitic neutron capture both negatively affects the neutron economy and also results in radioactive and volatile ¹⁴CO₂ or radioactive carbides that will increase the activity of the waste streams [20]. Since increased safety and retention of radioactive isotopes as well as improved economy is expected for ATFs, it has been suggested that the nitride fuel is made from the nitrogen isotope ¹⁵N instead which would prevent the parasitic neutron capture. However, natural nitrogen is composed of 99.64 % ¹⁴N which means that isolation of the much rarer ¹⁵N isotope would require expensive refinement facilities which there currently are none of in the world [27]. To compensate for the neutron loss, the enrichment of the UO₂ has to be increased from 4.2% to 4.5% according to estimations. However, if 50 or 90% ¹⁵N was used instead the enrichment level for the same burn-up would be 3.9 and 3.4% respectively [20].



1.1.6 UN Dopants

There have been different suggested approaches to improve the corrosion resistance of UN, one of which is making a composite material by doping the fuel with different metals. There are several metals and other elements that can potentially be used to improve the fuel. However, there are both downsides and upsides for these potential dopants that have to be considered before pursuing them [7].

Nickel, chromium and iron are metals that together are known for their corrosion resistant properties in various steel alloys. Iron and nickel both have a high cross sections for thermal neutrons resulting in significant neutron penalties should they be used in UN fuel. Titanium could potentially form passive oxide layers (TiO_2) but also have a large cross section. Interestingly, titanium can act as a way to remove carbon which could be useful for controlling carbon content during synthesis [27]; the importance of carbon content is explained in greater detail in the Theory chapter. Thorium has recently been shown to increase the oxidation resistance of UN pellets in air [20], although this study did not find any improved oxidation resistance in water compared to undoped UN. Thorium also have a considerable cross section that would absorb a significant portion of the available neutrons. However, the fertile isotope ^{232}Th can transmute to fissile ^{233}U via thermal neutron capture which helps to counteract the neutron penalty.

As mentioned, chromium is known for its use as an anti-corrosion agent in steels. Chromium(III) can form chromia (Cr_2O_3) which as an even oxide layer provides strong passivity in both air and water at high temperatures [28]. It is expected that an evenly distributed layer of Cr_2O_3 would successfully protect UN in standard reactor operating conditions. Chromium doped UN pellets have shown increased corrosion resistance in boiling water as the doped pellet remained intact for 5 hours of boiling while the pure UN reference collapsed after a few minutes. Aluminum(III) can also form a similar alumina (Al_2O_3) layer [28] which can provide protection at even higher temperatures (up to 1400 °C compared to Cr_2O_3 at 1000 - 1100 °C) [29]. In order for dopants to successfully be incorporated in a crystal matrix, the difference in radius compared to the dominant element must be less than 15%. Both aluminum and chromium have a difference of 16 and 18% of uranium respectively. However, these dopants can still be evenly distributed in the matrix which would result in the formation of passive oxide layers [27].

1.2 Aim and Limitations

The aim of this project is to produce UN with the added metal dopants aluminum and chromium in order to achieve improved corrosion resistance properties, and to study the effects these dopants have on the material.

Points of interest:

- Microstructure (cracking/porosity)
- Elemental composition
- Distribution of chromium and aluminum
- Crystal matrix and phases
- Oxidation performance

Some limitations of this project include:

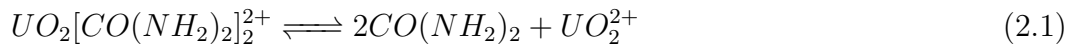
- The UN material synthesized will be made from natural uranium with a fissile content of 0.7%, since the material will only be used for studying chemical and material properties. As the enrichment of the uranium is irrelevant, natural uranium is used.
- This project will not focus on achieving low levels of oxygen and carbon contamination which are necessary for commercial production. Initial carbon content in the precursor solution is detrimental to achieve a balanced carbothermal reduction. This reaction allows the formation of UN. Thus, the synthesis will not be fine tuned for high purity and the amount of carbon lost in the washing process will not be measured, which would otherwise be necessary to investigate a high purity production route.
- The synthesized UN will not be pressed and sintered into fuel pellets which would otherwise be used to further investigate the properties of the material. This step is outside the scope due to time limitations.

2

Theory

2.1 Internal Sol-Gel Process

The internal sol-gel process or just "internal gelation process" (IGP) is based on the hydrolysis of a aqueous solution that is activated by heat. For the production of UN the solution used is a uranyl solution. This can be done by dropping the solution into a column of heated silicon oil, resulting in droplet sized gel microspheres. The active compounds during the gelation process are the gelling agent Hexamethylenetetramine (HMTA) and the complexation agent urea. The gelation process for a uranyl metal solution is described below [30][31]:



When the solution is heated the uranyl-urea complex is broken releasing uranyl ions (Reaction 2.1) which releases protons through hydrolysis (Reaction 2.2). The gelling agent HMTA is then protonated which causes further hydrolysis and increase of pH (Reaction 2.3), accelerating the reaction as more uranyl ions can hydrolyze and release more protons (Reaction 2.4). The purpose of adding urea is to keep the solution from initiating gelation prematurely by binding the uranyl ions in a complex which is stable as long as the solution is kept cool.

2.2 Reduction to UO_2

The UO_2 present in the gel-microspheres are higher oxides than UO_2 . Before the UN is formed, the microspheres are first reduced in an H_2 atmosphere after the gel microspheres have been completely dried in room temperature. The reduction is described below: [32]:



As steam is formed as a result of the reduction, carbon present in the material can be lost by formation of carbon monoxide [33]:

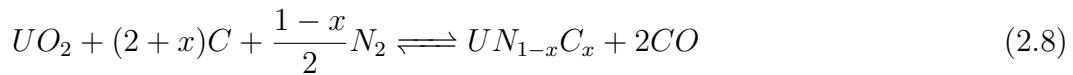


2.3 Carbothermal Reduction to UN

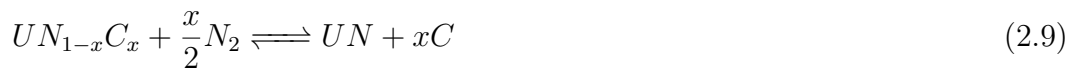
In order to form UN the UO_2 oxides in the microspheres are reduced at high temperatures using carbon as a reducing agent in a pure N_2 atmosphere. UN can also be produced by using a reducing atmosphere [27]. Below 1450 °C the nitride formation is described as [34]:



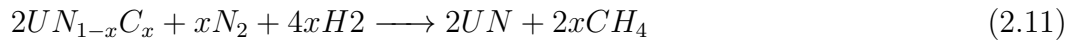
Above this threshold, carbonitrides begin to form instead:



These carbides can then theoretically be eliminated after prolonged treatment [3]:

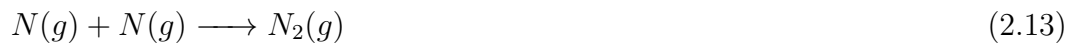
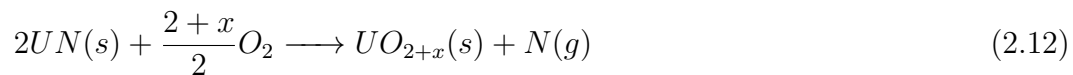


The carbonitrides and carbon can also be removed with added hydrogen gas [35]:

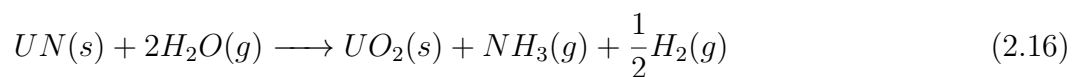
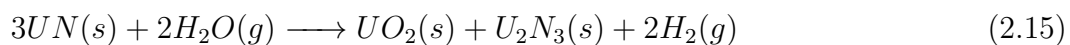


2.4 Oxidation and Hydrolysis of UN

A suggested oxidation sequence of UN in air has been suggested [36]. A thin layer of higher UO_{2+x} is instantaneously formed covering the entire surface of the sample (Reaction 2.12). Oxygen then chemisorbs into the oxide layer and diffuses into the sample, continuing the reaction. The liberated nitrogen is then either formed into N_2 gas or absorbed into UN forming higher nitrides (Reaction 2.13 and 2.16).



The hydrolysis of UN is reportedly similar to the oxidation except that the final product formed is UO_2 . It is argued that higher oxides - such as UO_3 and U_3O_8 which begin to form at 250 °C in air oxidation - are not formed because of the larger size of water molecules and the low oxidation potential.



2.5 Chemistry of Dopant Metals

As this project aims to produce UN with added chromium and aluminum, the reaction steps with these metals are investigated in this section. Hydrolysis of added chromium(III) and aluminum(III) should similarly to uranyl(II) produce respective hydroxides (Reaction 2.2) as both metals are easily hydrolysed. The aging step (explained in the Method chapter) where the microspheres are submerged into ammonium hydroxide should in theory ensure a complete hydrolysis of all three metal ions.

The carbothermal reduction of the dopant metal oxides are done similarly as the UO_2 in reaction 2.7 albeit with a different stoichiometry as the dopant metal ions are trivalent instead of divalent [38] [37]. Instead of UN, chromium nitride (CrN) and aluminum nitride (AlN) is formed instead. CrN is unstable above temperatures of 1000 °C which is much lower than the temperatures used for UN via carbothermal reduction which makes chromium evaporation inevitable at those temperatures [37].



3

Method

The production of UN microspheres can be divided into three steps. First, gel-microspheres are made from a uranyl solution via IGP. After the microspheres have been aged, washed and dried, they are reduced into UO_2 via heat treatment in a reductive atmosphere. The last step is similar to the second step but with higher temperatures, which allows the oxygen to be substituted with nitrogen via carbothermal reduction. After the production is done the properties of the microspheres are studied with various analytical equipment. The chemicals used are listed in the last section of this chapter.

3.1 Batch Profiles and Indexing

The doped batches will have 20% of their molar uranium content replaced with the dopant metals aluminum and/or chromium. All batches will be referenced by their name listed in Table 3.1. The prefix "UN" is changed when a precursor batch is referenced, for example $\text{UO}_2(20\text{-Al})$ or $\text{UO}_x(20\text{-Al})$. All batches will be duplicated for a total of 12 batches.

Table 3.1: Batch name and dopant profiles (% of total molar metal content)

Name	U	Al	Cr
UN(100-U)	100	0	0
UN(20-Al)	80	20	0
UN(15-Al/5-Cr)	80	15	5
UN(10-Al/Cr)	80	10	10
UN(5-Al/15-Cr)	80	5	15
UN(20-Cr)	80	0	20

3.2 Production of Gel-Microspheres

For the production of gel-microspheres a double jacketed beaker and column were used. The solution was prepared in the beaker and constantly stirred using a magnetic stirrer. The prepared solution was then dripped into silicon oil in the column using a plastic pipette. The rate of dripping was around two drops per second, fast enough to get small droplets, and slow enough to ensure that the droplets had enough leeway preventing them from merging. Column and droplets can be seen in Figure 3.1. The beaker and column were cooled and heated to 4 °C and 70 - 90 °C respectively using separate water baths and pumps. The column was 30 cm long and 5 cm in diameter. On average, the microspheres were left in the heated column around 10 min to ensure that the gel had solidified. The microspheres were collected using a sieve, washed, aged and finally dried in a fume hood at room temperature.

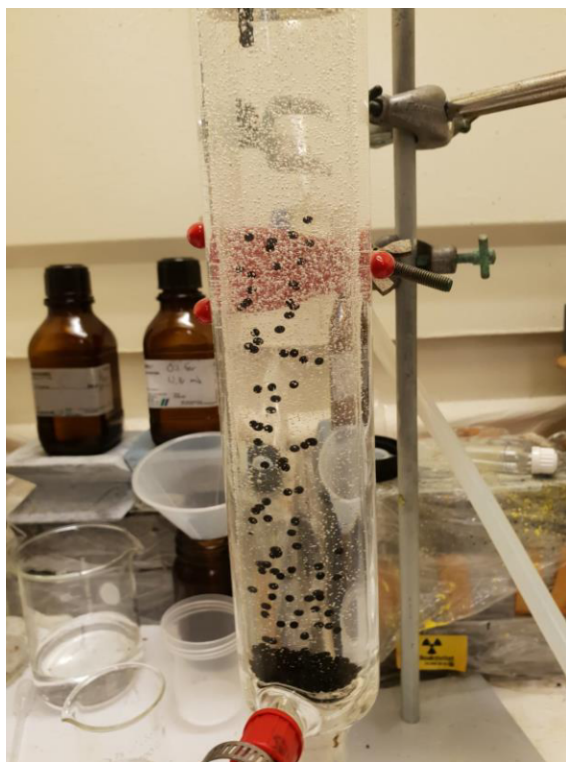


Figure 3.1: Uranyl solution droplets going through hydrolysis in a silicon oil filled column. Picture is taken from a previous study using the same equipment and setup [2].

The solutions were prepared in batches starting with 5 ml of 1.5 M uranyl solution diluted from a 1.9 M stock solution, which was prepared by dissolving uranyl nitrate crystals in purified water. The doped batches with varying aluminium and chromium content were prepared starting with 5 ml 1.2 M uranyl solution in which aluminum and chromium nitrate salts ($\text{Al/Cr}(\text{NO}_3)_3 \cdot 9 \text{H}_2\text{O}$) were added, resulting in equal metal content of 7.5 mmol in all batches including uranium. The remaining chemicals were then added in respect to the total molar metal content. Urea (x1.3) was added followed by HMTA (x1.7 pure/x1.8 doped) which was added in steps to prevent the formation of lumps. A non-ionic surfactant (5 drops) was then added before adding a carbon graphite powder (x2.5). The solution was stirred for 10 min to ensure even distribution of carbon before dripping the solution into the column. Since the doped microspheres are more difficult to gelate a higher column temperature was used (90 °C vs. 70 °C for pure batches). This is also why more HMTA was added; By adding additional HMTA and using higher temperatures gelation becomes easily achievable, the drawback being compromised microsphere structure in the form of embrittlement and cracks in the final product. The metal concentration of the solution was estimated to be around 1.1 M after considering the volumetric expansion caused by the added compounds.

The washing steps consisted of two 10 min washes in 50 ml petroleum ether using a 250 ml beaker which was periodically swirled around gently. The reason why two washes were used was due to significant silicon contamination observed in preliminary experiments. The aging step was done using 50 ml of ammonium hydroxide in the same beaker for 10 min to remove residual reactants and to complete the hydrolysis. A final 10 min wash with 50 ml purified water was done before letting the microspheres dry on a ventilated fume hood for 24 - 48 hours.

3.3 Reduction and Nitridation

The reduction and nitridation steps were done in a tube furnace (ETF 30-50/18-S). An alumina tube was inserted into the furnace and the sample was placed in the center of the tube in an alumina crucible. Gas valves were placed at the two ends of the tube and connected to the gas system. Before turning on the heating program the tube was flushed with the reaction gas (5% H_2 / 95% N_2) at a flow of 3 L/min for 20 - 30 min in order to flush all oxygen. Different alumina tubes were used for reduction and nitridation as high levels of carbon is released during nitridation which causes significant accumulation of soot inside the tube. During reductions which are done at a much lower temperature two samples were done simultaneously. The temperature gradient is much steeper at higher temperatures which is why the nitridation is limited to only one crucible each run. The crucibles were retrieved with a metal wire and the UN samples were immediately put into a glovebox with minimal oxygen content.

3. Method

The reduction program starts with a temperature ramp at 3 °C/min to minimize the formation of cracks, and is kept at 350 °C for one hour to remove excess water in the microspheres. The program then ramps up to 800 °C at 5 °C/min where the reduction took place over 2 hours. The program then cools down at 10 °C / min to room temperature. However, at around 900 °C the heat loss of the sample becomes slower than the program, meaning the actual cooling time takes several hours longer.

The nitridation program ramps up to 1550 °C at 10 °C and stays there for 5 hours before ramping down to room temperature at 10 °C. A shorter second step at 1650 °C could be added to the program the further decarbonize the microspheres but is avoided as an attempt to prevent evaporation of chromium. The gas is switched from (5% H₂ / 95% N₂) to pure argon 10 min before the final cooling step. This is to prevent the formation of U₂N₃.

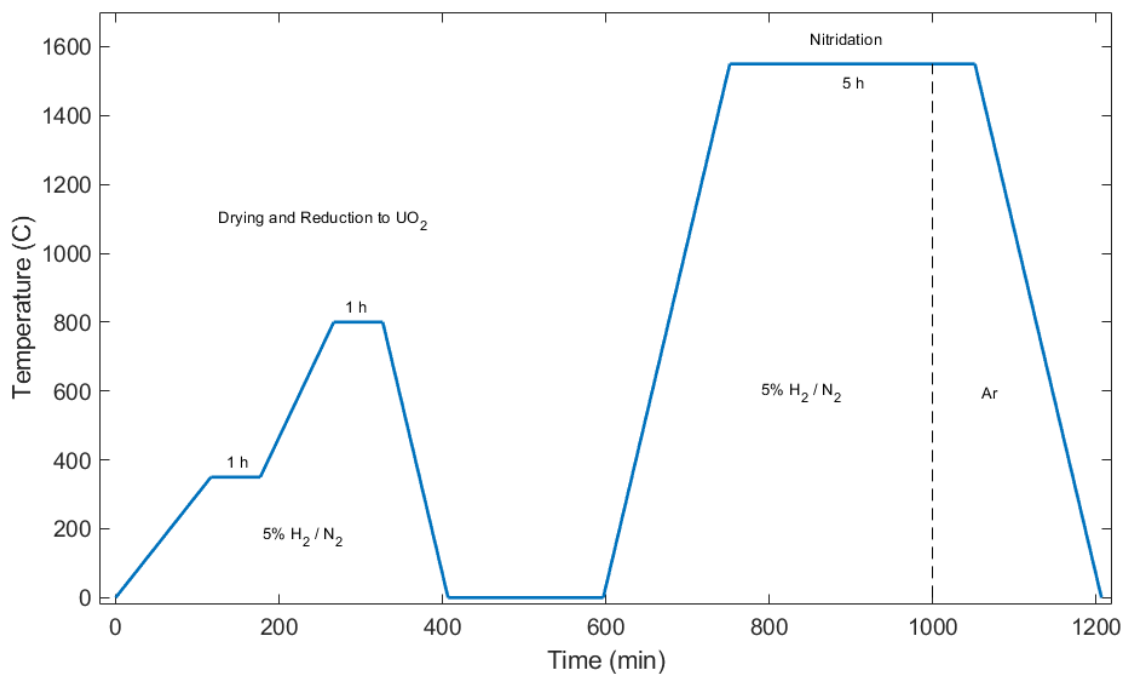


Figure 3.2: Temperature profile for reduction and nitridation programs.

3.4 Analytical Instruments and Procedure

This section explains all analytical equipment and procedures used to analyze the product. SEM/EDX and XRD analysis were done inside gloveboxes with minimal oxygen content ($\text{PO}_2 < 1$ ppm). The other were done in regular lab conditions.

3.4.1 SEM/EDX

A tabletop scanning electron microscopy (SEM) machine with energy dispersive x-ray (EDX) was used to investigate the surfaces of the microspheres and to confirm the presence of doped metals and any contaminants like silicon from the gelation process. A SEM image is produced by detection of secondary electrons emitted as a result of excitation of the target atoms hit by the high intensity electron beam, which ranges from 5 - 15 kV. The chemical characterization image is based on characteristic x-rays emitted when an electron goes through deexcitation after a lower electron has been ejected by the incident electron beam. The energy of the resulting x-ray is then represented by the energy difference from the electron shells involved in the deexcitation.

3.4.2 XRD

X-ray diffraction (XRD) analysis was performed using a Bruker D2 Phaser XRD instrument. The UN microspheres were thoroughly ground up into a fine powder and evenly distributed on the XRD disc. The disc was then inserted into the instrument which performed the analysis using a Cu ($\lambda = 1.54184 \text{ \AA}$) radiation source at a 2θ range of 20° - 144° . The current and voltage was set to 30 kV and 10 mA. The crystal lattice parameter is determined using the known miller indices representing the crystallographic plane, the wavelength and the angle of the peaks shown in the diffractograms. The peaks are caused as a result of constructive interference as the incident x-rays are emitted at certain angles. The resulting peaks can then be compared to reference diffractograms to confirm the crystal structure of the samples.

3.4.3 ICP-MS

The metal contents (uranium, chromium and aluminum) were measured using an inductively coupled plasma mass spectrometry (ICP-MS). The instrument used was an iCAP Q (Thermo Scientific). The samples were dissolved in aqua regia made from hydrochloric and nitric acid, filtered and diluted to the calibration range (1-50 ppb) with 0.5 M nitric acid. The solution is steadily pumped into the ICP-MS where it is nebulized and carried into a plasma torch with argon gas. The plasma is generated through oscillating magnetic fields and is then transferred into a quadrupole where the species are separated based on the ionic mass-to-charge ratio. The metal contents of the samples can then be determined as they are proportional to the detection signal.

3.4.4 Carbon, Oxygen and Nitrogen Analysis

The carbon content of the batches was measured using a LECO CS744 instrument. The samples were weighed (~ 50 mg) in disposable alumina crucibles together with an accelerant. Blanks and references (steel pellets) were also prepared for calibration. The crucibles were then placed into the instrument which then incinerated the samples. The CO_2 produced from the carbon present in the samples were then continuously measured using an infrared detector to determine the total carbon content. Oxygen and nitrogen content was measured using a LECO TC-436DR instrument. The samples were placed inside tin foil (not aluminum) boat which was then inserted into a nickel crucible. The crucible was then inserted and incinerated. The nitrogen is then determined by measuring changes in conductivity of the helium carrier gas. Oxygen reacts with the crucible and is converted to CO_2 which is measured by non-dispersive infrared cells.

3.4.5 TGA

Thermogravimetric analysis (TGA) was done using a Q-500 (TA Instruments) to investigate the oxidation of some of the batches. The samples were placed in an alumina basket mounted with a platinum wire. The mass change of the samples were then measured over several hours and analyzed using Universal Analysis (TA Instruments).

3.5 Chemicals

Chemical	Manufacturer	Use
Purified water (Milli-Q)	Merck	Aqueous solvent
Carbon black (MOGUL L)	CABOT	Reducing agent
HMTA 99% pure	Sigma Aldrich	Gelling agent
Solid urea 99% pure	Sigma Aldrich	Complexation agent
Triton X	Sigma Aldrich	Non-ionic surfactant
Petroleum ether	Alfa-Aesar	Organic solvent
Ammonium hydroxide 30%	Sigma Aldrich	Reducing agent
Chromium nitrate	Sigma Aldrich	Dopant
Aluminum nitrate	Sigma Aldrich	Dopant
Nitric acid	Merck	Aqua regia reagent
Hydrochloric acid	Sigma Aldrich	Aqua regia reagent

4

Results and Discussion

In this chapter all analytical data is reviewed as well as the hydrolysis, washing and reduction procedures.

4.1 Synthesis, Microstructure and Elemental Distribution

The dopant profile had a clear effect on the microstructure with the UN(100-U) batches being the least porous and cracked. Figure 4.1 shows a UN(100-U) microsphere with ideal shape and surface except some visible silicon contamination appearing as dark spots, confirmed by EDX. Unsurprisingly, silicon contamination could also be found in all other batches as the same washing procedure was used on all of them. These spots registered as aluminum because of the overlap of silicon and aluminum on the EDX spectrum. Since the spots also appear on the UN(100-U) samples and does not seem to respond to aluminum concentration, it is concluded that these spots are in fact silicon. The washing process did not only leave residue silicon but also caused significant carbon leaching which made the carbon content impossible to control in the final microspheres. Most leaching was observed in one of the 20-Al batches and one of the 20-Cr batches. This 20-Cr batch was discarded due to severe cracking and disintegration after the nitridation process. The leaching observed was inconsistent and without following any clear patterns. It should be noted that the amount of leaching was determined visually and not through measurement of carbon content in the leachate which can be done using total organic carbon (TOC) analysis. As the entire gelation- and washing processes are manual it is possible that inconsistencies in the procedure affected the amount of carbon leached. The most inconsistent variable was the time the microspheres spent inside the column, which was not measured precisely. It remains unclear whether or not this is the cause of the increased leaching.

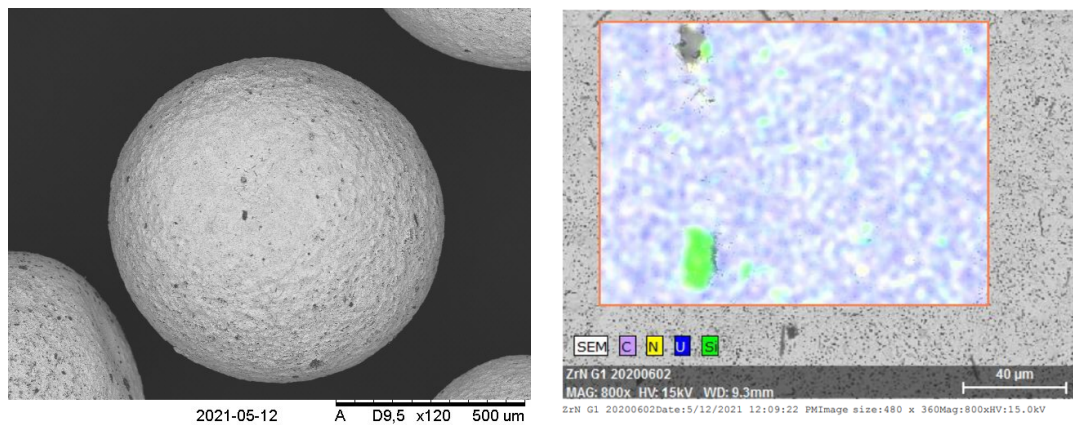


Figure 4.1: SEM/EDX image of a UN(100-U) microsphere with visible silicon contamination.

The most apparent effect of increased chromium concentration was the embrittlement of the microspheres which can be seen in Figure 4.2. The same phenomenon was observed in an earlier study [20] where the increased embrittlement was attributed to the different behaviour of chromium in the gelation process compared to uranyl which it replaces. Cracking could be a result of unwashed reactants forming gaseous compounds escaping during heat treatment which could have been exacerbated by the addition of dopant metals. Another probable cause is the fact that chromium is easily evaporated, which means more cracking due to increased gas development. Chromium evaporation will be reviewed in greater detail in the ICP-MS section.

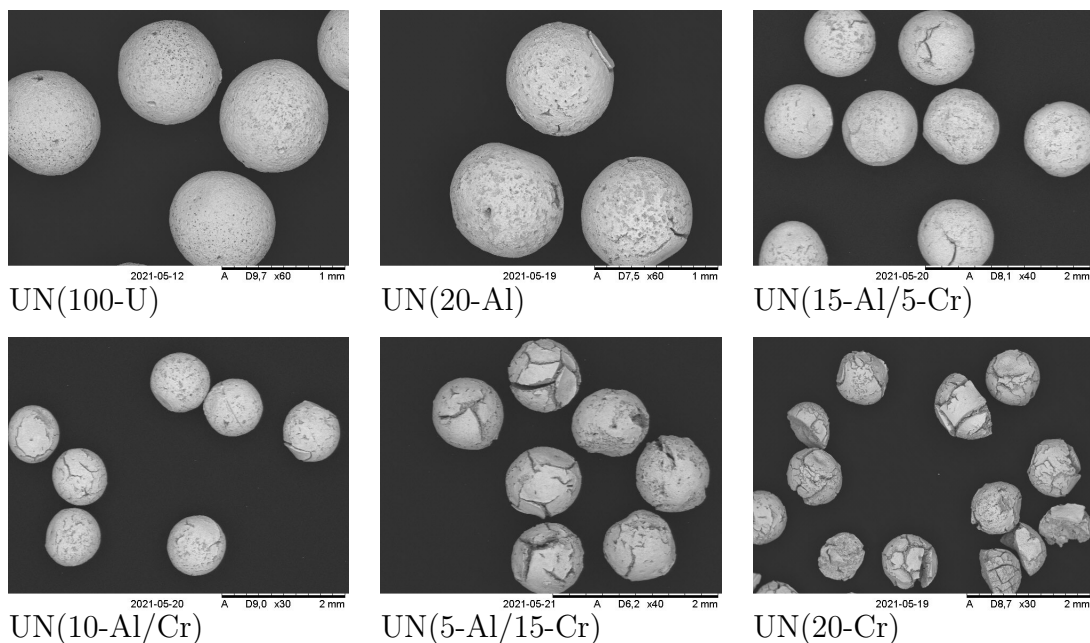


Figure 4.2: SEM images of UN samples with increasing chromium concentration.

All microspheres had some level of porosity that increased with aluminum content. Figure 4.3 shows how the surface porosity of the UN(20-Cr) sample were minimal where no aluminum is present. This phenomenon could be explained by aluminum accumulating along the grain boundaries in the UN matrix as theorized by Mishchenko et al [7]. This could possibly reduce the adhesion between grain boundaries, resulting in increased porosity.

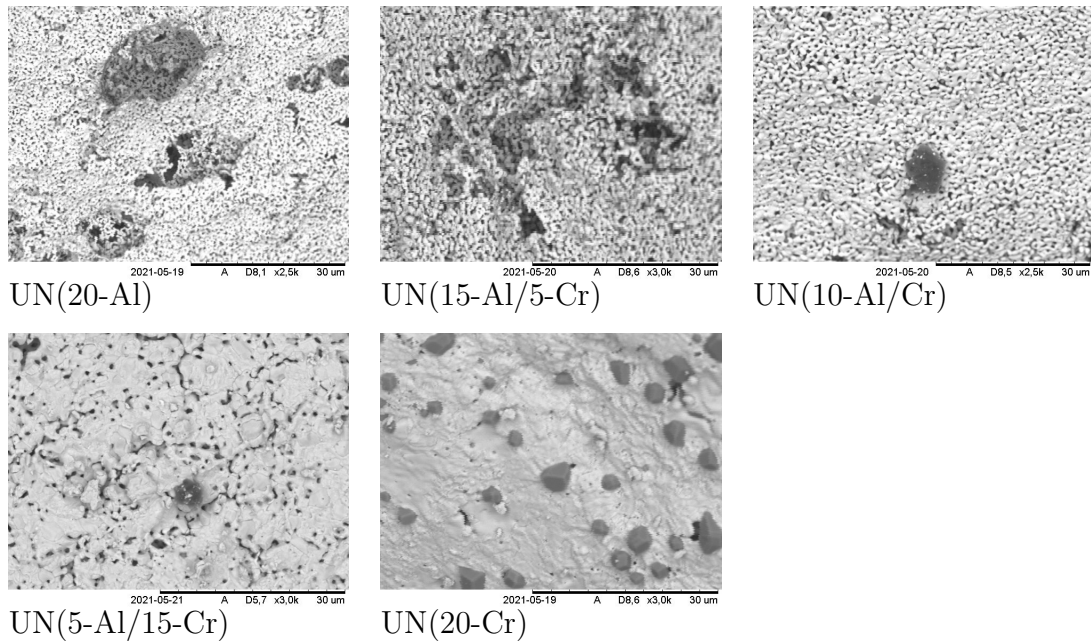


Figure 4.3: SEM images of UN samples with increasing chromium concentration.

Judging from the EDX image of a UN(20-Cr) sample (Figure. 4.4) the chromium seems evenly distributed. Pebble-like formations were found on the surface of all UN(20-Cr) microspheres, but never on microspheres with lower chromium concentration, suggesting that these formations are based on precipitated chromium. This would align with a previous study [2] where chromium agglomerations were confirmed at higher chromium concentrations due to the limited solubility of chromium in the UN phase. The reason why these formations appear invisible on the chromium EDX-image is most likely because the instrument was poorly calibrated during analysis. Another possible explanation is that the chromium has evaporated after the agglomerations formed.

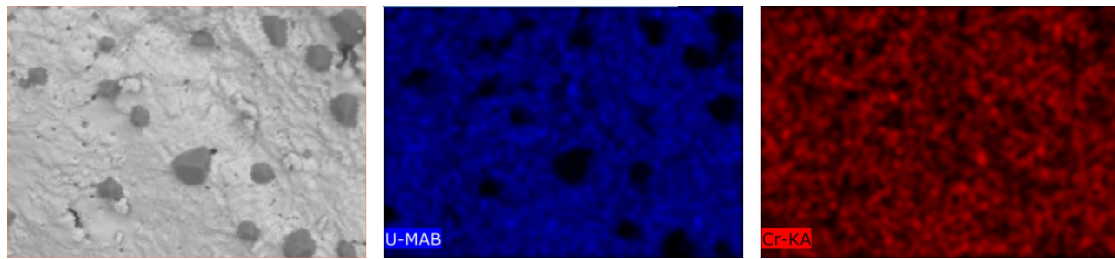


Figure 4.4: EDX image of crystalline formations on a UN(20-Cr) microsphere.

All other elements present (Al, N, O, C, U) appeared evenly distributed. Carbon, oxygen and nitrogen are all adjacent on the EDX-spectrum with significant overlap which makes it difficult to precisely determine the distribution of said elements. As discussed earlier in this section, large spots could be found that were asserted to be silicon contamination. However, some smaller spots appeared on the 20-Al samples that were invisible on the SEM-images. These spots can be seen in Figure 4.5 and are most likely concentrated aluminum as they did not appear at lower aluminum concentrations.

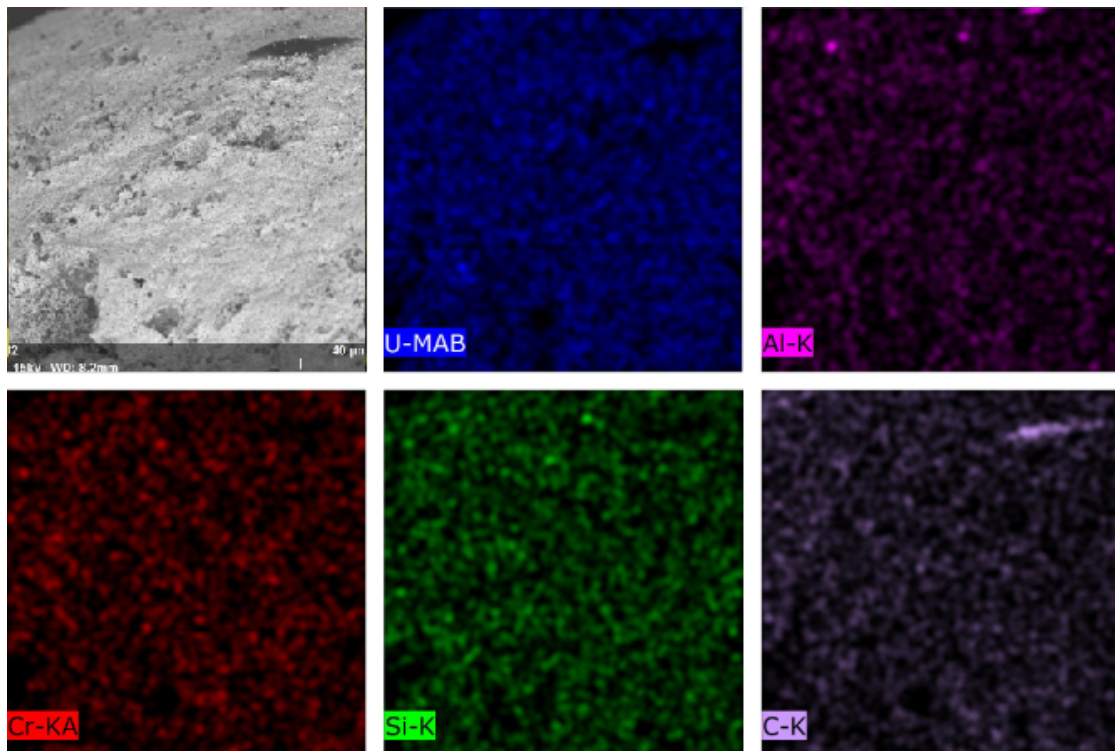


Figure 4.5: EDX image of a UN(20-Al)-C microsphere with different elements labeled.

4.2 Carbon, Oxygen and Nitrogen Analysis

The elemental composition of the final uranium nitride is crucial to determine the overall quality of the fuel. By comparing the actual nitrogen content to the theoretical content, as well as observing the level of impurities (carbon and oxygen) it is possible to review the adequacy of the original gel composition and the reduction process. Carbon is added to enable the carbothermal reduction which is used to substitute oxygen with nitrogen (Reaction 2.7). Original carbon content is thus key to balance the final composition.

In Table 4.1 the carbon, oxygen and nitrogen content of the final UN microspheres are listed. As the carbon content is near zero and the oxygen content is significant, it is concluded that the carbothermal reduction was incomplete due to inadequate carbon content. This is confirmed by the gap between the actual and theoretical nitrogen content. The carbon content could simply be increased by adding more graphite powder to the gel solution, or by reducing the amount lost in the washing process due to leaching. In this study, carbon content is not measured before the last reduction step which would otherwise be crucial for investigating the reduction process in terms of carbon contamination, which is outside the scope.

The oxygen content also suggests that the carbothermal reduction was incomplete, although some of it could have come from the atmosphere during transportation between gloveboxes. The nitrogen content is lower in samples that contain chromium. This means that chromium either is not present which means there is no chromium to bind any nitrogen, or that the chromium is present as pure chromium or interstitially in the UN phase.

Table 4.1: Elemental composition (wt%) for all batches. Values are averaged across duplicate batches. (* one batch only) (** theoretical content)

Composition	C	O	N	N**
UN(100-U)	0.021±0.009	0.591±0.004	5.24±0.03	5.56
UN(20-Cr)*	0.014±0.004	0.690±0.006	5.099±0.016	6.52
UN(15-Cr/5-Al)	0.015±0.007	0.628±0.022	5.40±0.08	6.56
UN(10-Cr/Al)	0.015±0.005	0.632±0.006	5.8±0.3	6.59
UN(5-Cr/15-Al)	0.011±0.008	0.950±0.0023	5.97±0.14	6.63
UN(20-Al)	0.028±0.008	0.912±0.004	6.18±0.25	6.67

4.3 XRD

XRD analysis was done on all batches and the duplicates were near identical. The graphs below only display data from the duplicate sample with highest intensity, which was the only observed difference. All patterns showed distinct peaks corresponding to UN, indicating a dominant UN matrix which was expected. Figure 4.6 shows a UN(100-U) pattern next to a simulated UN pattern with potential UO_2 peaks marked in the sample pattern. These UO_2 peaks were found in all samples which can be seen in Figure 4.7.

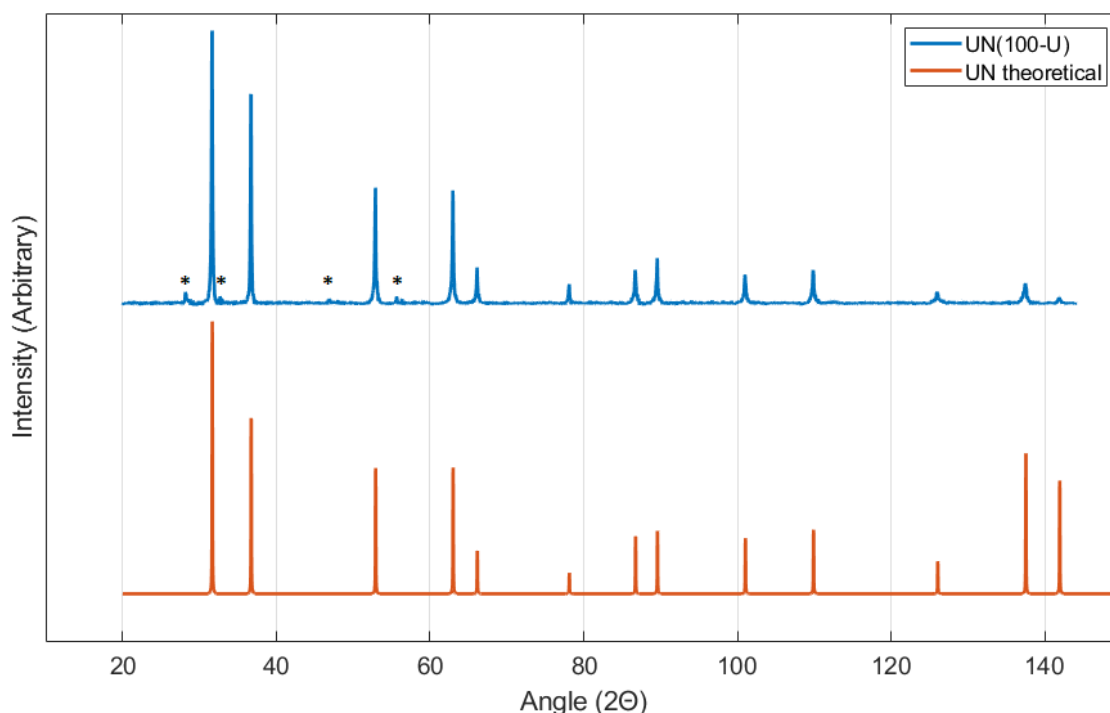


Figure 4.6: Comparison of XRD patterns between a UN(100-U) sample and simulated UN. Patterns are normalized against highest peak. Potential UO_2 peaks are marked with an asterisk (*).

The lattice parameters for all doped species were 4.89 Å except UN(20-Cr) which had a parameter of 4.91 Å. As seen in Figure 4.7, the corresponding pattern is visibly shifted to the left and also have the highest UO_2 peaks. It is not clear what is causing this shift as there does not seem to be a link between elemental content like carbon or chromium (see ICP-MS section for chromium content). The presence of a more dominant UO_2 phase should not cause a shift of the UN phase to the left. No chromium or aluminum phases could be observed in the XRD-patterns. There could still be such phases present if they are below $\sim 5\%$ of total weight or randomly oriented - meaning they would not appear on the patterns.

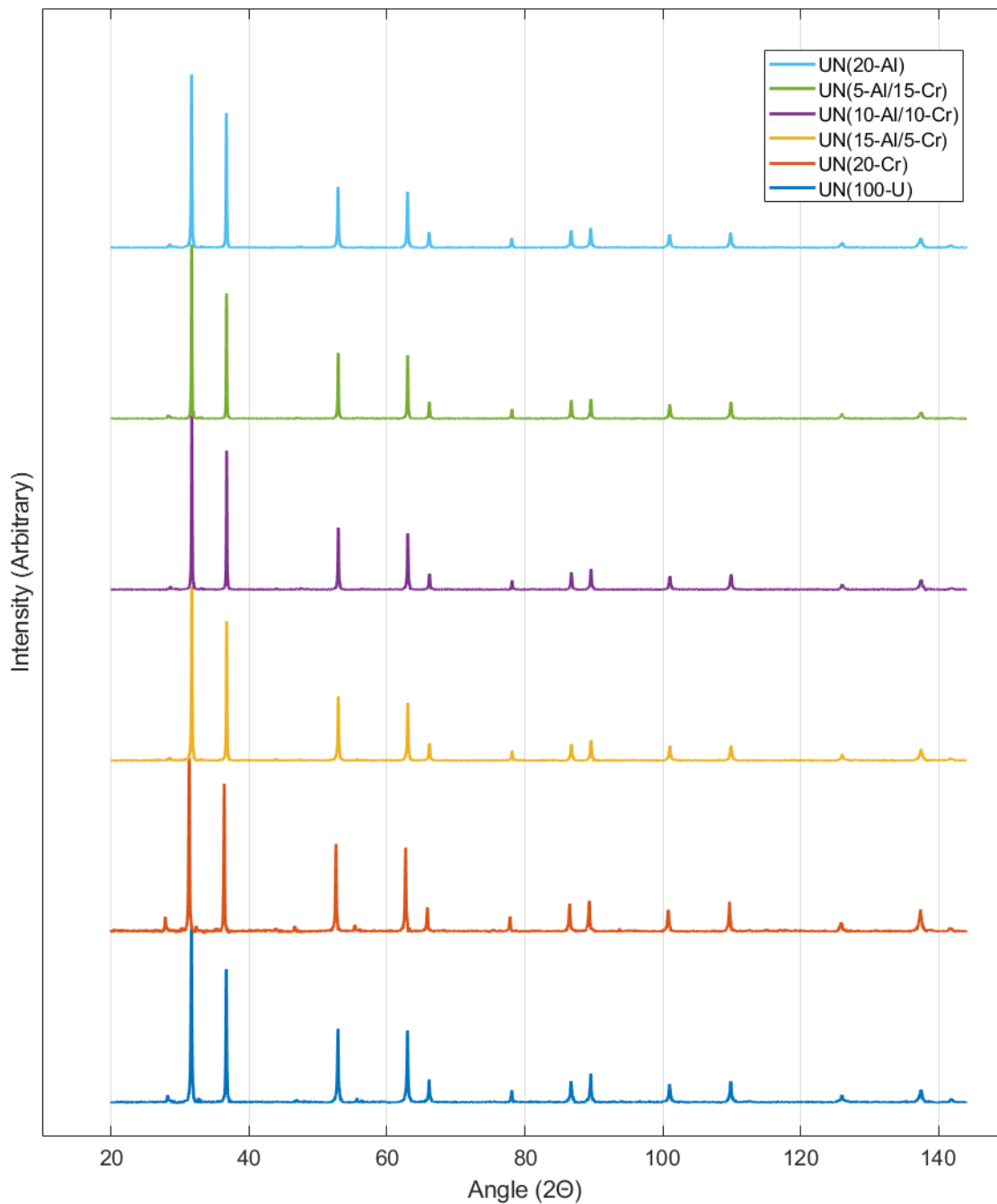


Figure 4.7: Comparison of XRD patterns of all UN batches. Patterns are normalized against the highest peak.

4.4 ICP-MS

The molar ratio of chromium to the total metal content is shown below in Table 4.2. The aluminum data was omitted as its measured content was too high ranging from 27 to 55% for all samples measured, including those without any added aluminum. This faulty data was determined to be a result of equipment failure and possibly contamination. The actual aluminum contents remain unknown. It should be noted that all compositional data was calculated by dividing the molar content of respective metal by the total molar metal content (chromium, aluminum and uranium). This means that the faulty aluminum data also affects the chromium data.

In theory, the chromium contents displayed in Table 4.2 for UO_x should match the composition of the batch name since no chromium could have evaporated before heat treatment. The chromium contents for the UO_x batches are all in somewhat reasonable range except for $UO_x(100-U)$ and $UO_x(20-Al)$ which should not contain any chromium whatsoever. The $UO_x(20-Al)$ data was omitted from the Table 4.2 as it had extremely unreasonable chromium contents of 10 and 18 %.

The contents for the UO_2 batches are similar to to the UO_x batches and show a slight drop in content due to chromium evaporation caused by the low temperature treatment (800 °C). As for the UN samples the chromium content drops significantly to 3 - 6%, either as a result of significant evaporation caused by the high temperature treatment (1550 °C), or difficulties in dissolving CrN in aqua regia, most likley both.

The last reduction program was changed by removing the decarbinization step, thus lowering the maximum temperature from 1650 to 1550 °C in order to prevent excessive chromium evaporation. It is not possible to say if this temperature reduction have preserved any significant amounts of chromium, but it should in theory somewhat have reduced evaporation.

Table 4.2: Mole% of chromium to total metal content of doped batches after each step of the production process - hydrolysis, reduction, and nitridation. Values are averaged across duplicate batches. (* one batch only)

Batch Name	UO_x	UO_2	UN
100-U	5.5	4	4
20-Cr*	20	17	3
5-Al/15-Cr	16	15	5
10-Al/Cr	12	11	6
15-Al/5-Cr	8	7	5

4.5 TGA

In order to investigate the oxidation of batches in air, thermogravimetric analysis was done on four samples with different dopant profiles seen in Figure 4.8. The TGA-curve looks similar for all samples with a slow mass gain at lower temperatures and a rapid gain in mass thereafter. This point of accelerated growth is referred as the onset temperature, which is defined as the temperature where the rate of mass gain is more than 5% of the final mass gain [20]. Once the maximum gain is reached the curve plateaus as the material is fully oxidized. At higher temperatures all samples except UN(100-U) show a further mass increase albeit slower. This gain could possibly be attributed to oxidation of residual doped species that have remained unreacted up until a high temperature threshold, which was reached around 700 °C. The UN(100-U) sample is showing a slight decrease in weight which has been attributed to the release of nitrogen from UN_xO_y intermediate species [39].

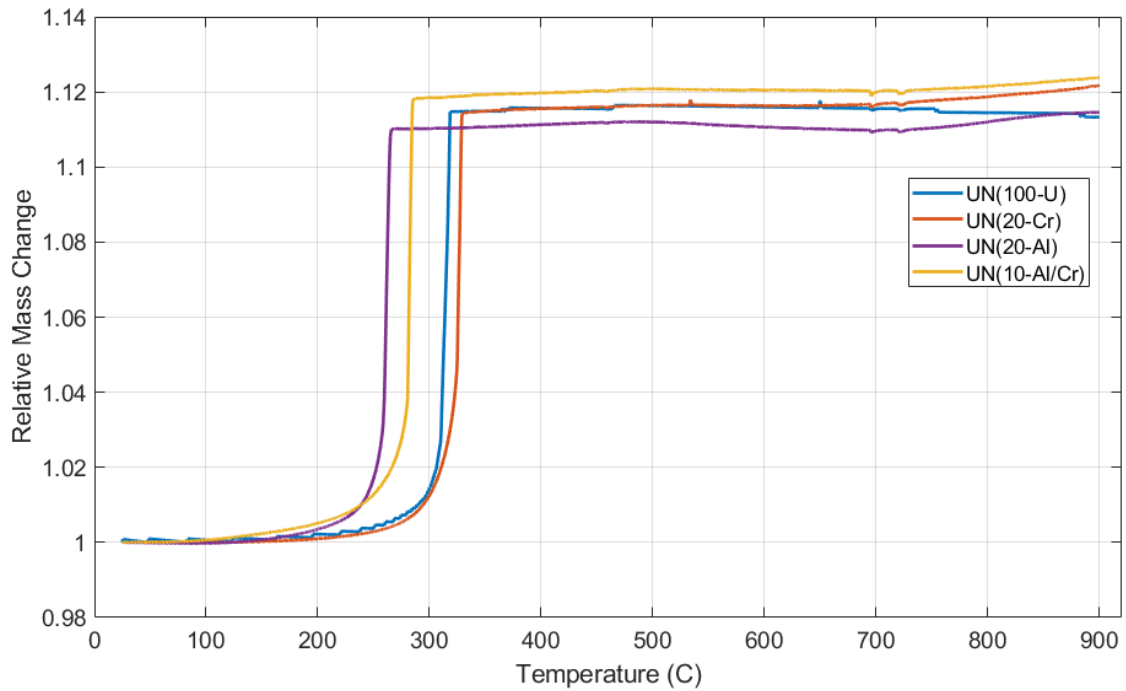


Figure 4.8: Relative change in weight of different UN batches plotted against time in seconds.

In Table 4.3 the onset and peak reaction rate temperatures can be found. The UN(20-Cr) sample had the highest onset peak reaction temperature at a few degrees above UN(100-U). The samples containing aluminum had a clear reduction, with the 20-Al sample having the lowest temperatures. These results are in agreement with Mishchenko et al. [7] where added aluminum to UN pellets correspond to lower onset temperature and added chromium to higher onset temperature. It is suggested that the lower oxidation performance is a result of an increased surface area due to microstructural cracks formed by the difference in thermal expansion between the UN and AlN phases. The high porosity of the aluminum rich microspheres clearly suggest that increased surface area is the cause of lower oxidation performance. It remains unclear what is causing the difference in mass gain between the species as no clear pattern can be observed.

Table 4.3: Onset- and peak reaction rate temperature ($^{\circ}\text{C}$) of different UN batches.

Dopant Profile	Onset	Peak
100-U	306	315
20-Cr	316	327
10-Cr/Al	276	282
20-Al	252	262

5

Conclusion

Adding both aluminum and chromium had a clear structural impact on the final UN microspheres. Chromium caused large scale cracking and disintegration which is believed to be due to the release of gasses, either from the evaporated chromium itself or disintegration of residual compounds. These hypothetical compounds could possibly be a result of changes in the hydrolysis behavior due to the different nature of chromium and uranyl ions. Moreover, the distinct pebble-like formations found on the surface of UN(20-Cr) microspheres were identified as precipitated chromium compounds caused by the limited solubility of chromium in UN. The increased surface porosity observed was hypothesised to be the result of aluminum distribution within the crystal matrix, causing lower adhesion between grains, as aluminum is accumulated at the boundaries. Small aluminum agglomerations could be found on the surface of the UN(20-Al) microspheres suggesting that a solubility limit has been reached similarly to chromium.

ICP measurements showed a clear trend where chromium contents were reduced after each reduction step, with the last high temperature step at 1550 °C showing the most significant drop. This confirms that chromium is evaporating. It was also found that CrN does not easily dissolve in aqua regia which means that some of the lost chromium most likely is a measuring error.

The TGA curves were in line with previous studies. The undoped batches showed a slight decrease in weight after around 700 °C which is caused by the release of nitrogen from intermediate UN_xO_y species. The increased weight observed in doped batches at around 700 °C is hypothesized to be caused by oxidation of dopant species that remain stable up until said temperature. Chromium increased onset temperature and aluminum reduced onset temperature, which is in agreement with previous studies. The lower performance of the UN(20-Al) batches is attributed to the large surface area which is either caused by the porous structure and/or microstructural cracks formed by a difference in expansion coefficient between the different phases.

6

Future Work

ICP measurements should be redone to study the aluminum contents. Because of the solubility issues with chromium in aqua regia, other methods should be used for aluminum analysis, e.g. X-ray Fluorescence (XRF). Better ICP data is needed for a more thorough review of microstructural impact and oxidation performance. Since the chromium data lacked precision, it would be beneficial to make a comparison between a 1550 and 1650 °C reduction pathway to ensure if the temperature difference affects final chromium content. A better washing method is needed that avoids silicon contamination and minimizes carbon leaching. If leaching is studied, TOC analysis of the leachate could be done to quantify the carbon lost. It would also be beneficial to study whether or not time spent in gelation column is related to microstructure and leaching. If a greater range of batches in terms of composition could be analyzed with TGA, more could be learned about the relationship between dopants and oxidation temperatures. The high temperature weight gain of doped batches could also be investigated to see if residual compounds are present. If high quality microspheres with known composition can be produced, the next step would be pressing and sintering the product into pellets for further research.

Bibliography

- [1] IAEA. Accident Tolerant Fuel Concepts for Light Water Reactors. (2014). www-pub.iaea.org/MTCD/Publications/PDF/TE1797web.pdf
- [2] Gonzalez Fonseca, L., Hedberg, M., Huan, L., Olsson, P. and Retegan Vollmer, T., 2020. Application of SPS in the fabrication of UN and (U,Th)N pellets from microspheres. *Journal of Nuclear Materials*, 536, p.152181.
- [3] Ekberg, C., Ribeiro Costa, D., Hedberg, M. and Jolkkonen, M. (2018). Nitride fuel for Gen IV nuclear power systems. *Journal of Radioanalytical and Nuclear Chemistry*, 318(3), 1713-1725.
- [4] Dell R, Wheeler V. The ignition of uranium mononitride and uranium monocarbide in oxygen. *Journal of Nuclear Materials*. 1967;21(3):328-336.
- [5] Johnson K, Ström V, Wallenius J, Lopes D. Oxidation of accident tolerant fuel candidates. *Journal of Nuclear Science and Technology*. 2016;1-7.
- [6] Insulander Björk K, Herman A, Hedberg M, Ekberg C. Scoping Studies of Dopants for Stabilization of Uranium Nitride Fuel. *Nuclear Science and Engineering*. 2019;193(11):1255-1264.
- [7] Mishchenko Y, Johnson K, Wallenius J, Lopes D. Design and fabrication of UN composites: From first principles to pellet production. *Journal of Nuclear Materials*. 2021;553:153047.
- [8] Vaidya V, Mukherjee S, Joshi J, Kamat R, Sood D. A study of chemical parameters of the internal gelation based sol-gel process for uranium dioxide. *Journal of Nuclear Materials*. 1987;148(3):324-331.

- [9] NUCLEAR 101: How Does a Nuclear Reactor Work? Energy.gov. 2021. www.energy.gov/ne/articles/nuclear-101-how-does-nuclear-reactor-work
- [10] Poston J. Do transuranic elements such as plutonium ever occur naturally? Scientific American. 1998. www.scientificamerican.com/article/do-transuranic-elements-s/
- [11] MOX, Mixed Oxide Fuel - World Nuclear Association World-nuclear.org. 2017. world-nuclear.org/information-library/nuclear-fuel-cycle/fuel-recycling/mixed-oxide-fuel-mox.aspx
- [12] Uranium Enrichment | Enrichment of uranium - World Nuclear Association. World-nuclear.org. 2020. world-nuclear.org/information-library/nuclear-fuel-cycle/conversion-enrichment-and-fabrication/uranium-enrichment.aspx
- [13] Choppin G, Liljenzin J, Rydberg J, Ekberg C. Radiochemistry and nuclear chemistry, fourth edition. Kidlington, Oxford, UK: Academic Press; 2013.
- [14] J.M.K.C. Donev et al. (2021). Energy Education - CANDU reactor [Internet]. Energyeducation.ca/encyclopedia/CANDUreactor.
- [15] Fast Neutron Reactors | FBR - World Nuclear Association. World Nuclear Association. 2021. world-nuclear.org/information-library/current-and-future-generation/fast-neutron-reactors.aspx
- [16] Cladding. nrc.gov. 2021. www.nrc.gov/reading-rm/basic-ref/glossary/cladding.html
- [17] Fukushima Daiichi Accident. World Nuclear Association. 2021. [Internet]. world-nuclear.org/information-library/safety-and-security/safety-of-plants/fukushima-daiichi-accident.aspx
- [18] QIN W, NAM C, LI H, SZPUNAR J. Tetragonal phase stability in ZrO₂ film formed on zirconium alloys and its effects on corrosion resistance. Acta Materialia. 2007;55(5):1695-1701.
- [19] hukla S, Seal S. Thermodynamic Tetragonal Phase Stability in SolGel Derived Nanodomains of Pure Zirconia. The Journal of Physical Chemistry B. 2004;108(11):3395-3399.

-
- [20] Gonzalez Fonseca, L. Advances in Accident Tolerant Fuel Research by Doping of Uranium Nitride. Thesis of Licentiate Degree of Engineering. 2020. Chalmers University of Technology
- [21] Youinou G, Sen R. Impact of Accident-Tolerant Fuels and Claddings on the Overall Fuel Cycle: A Preliminary Systems Analysis. Nuclear Technology. 2014;188(2):123-138.
- [22] Nuclear Fuel Fabrication - World Nuclear Association. World Nuclear Association. 2021. world-nuclear.org/information-library/nuclear-fuel-cycle/conversion-enrichment-and-fabrication/fuel-fabrication.aspx
- [23] Burkes, D., Mickum, G. and Wachs, D., 2010. Thermophysical Properties of U-10MO Alloy. Washington, D.C.: United States. National Nuclear Security Administration, p.7.
- [24] Hayes, S., Thomas, J. and Peddicord, K., 1990. Material property correlations for uranium mononitride. Journal of Nuclear Materials, 171(2-3), pp.289-299.
- [25] White, J., Nelson, A., Dunwoody, J., Byler, D., Safarik, D. and McClellan, K., 2015. Thermophysical properties of U₃Si₂ to 1773 K. Journal of Nuclear Materials, 464, pp.275-280.
- [26] Thermal Conductivity of Uranium Dioxide. Nuclear-power.com. 2022. [Internet] www.nuclear-power.com/nuclear-engineering/heat-transfer/thermal-conduction/thermal-conductivity/thermal-conductivity-of-uranium-dioxide/
- [27] Sajdova A, ACCIDENT-TOLERANT URANIUM NITRIDE. Thesis of Licentiate Degree of Engineering. 2018. Chalmers University of Technology
- [28] Herman A, Ekberg C. A Uranium Nitride Doped with Chromium, Nickel or Aluminum as an Accident Tolerant Fuel. Research & Reviews: Journal of Material Sciences. 2017;05(06).
- [29] M.P. Brady, I.G. Wright, B. Gleeson, Alloy design strategies for promoting protective oxide-scale formation, J. Occup. Med. 52 (2000) 16-21

- [30] COLLINS J, LLOYD M, FELLOWS R. The Basic Chemistry Involved in the Internal-Gelation Method of Precipitating Uranium as Determined by pH Measurements. *Radiochimica Acta*. 1987;42(3).
- [31] Vaidya V. Status of sol-gel process for nuclear fuels. *Journal of Sol-Gel Science and Technology*. 2008;46(3):369-381.
- [32] Ledergerber G, Kopajtic Z, Ingold F, Stratton R. Preparation of uranium nitride in the form of microspheres. *Journal of Nuclear Materials*. 1992;188:28-35.
- [33] Mukerjee S.K. Carbothermic reduction of (UO₂ + C) microspheres to (UO₂ + C) microspheres. *Journal of Nuclear Materials*. 1993;199:247-257.
- [34] Mukerjee S, Dehadraya J, Vaidya V, Sood D. Kinetics of the carbothermic synthesis of uranium mononitride microspheres. *Journal of Nuclear Materials*. 1991;185(1):39-49.
- [35] Bardelle P, Warin D. Mechanism and kinetics of the uranium-plutonium mononitride synthesis. *Journal of Nuclear Materials*. 1992;188:36-42.
- [36] Rao G, Mukerjee S, Vaidya V, Venugopal V, Sood D. Oxidation and hydrolysis kinetic studies on UN. *Journal of Nuclear Materials*. 1991;185(2):231-241.
- [37] Morita, S., Shimizu, H. and Sayama, Y., 2001. Synthesis of Chromium Nitride Powder by Carbo-thermal Nitriding. 15th International Plansee Seminar, 2, pp.139 - 151.
- [38] Li, F., Liang, Q., Jingwu, Z., Yao, Y., Wangchang, L., Shenglei, C. and Jing, Y., 2018. Phase, microstructure and sintering of aluminum nitride powder by the carbothermal reduction-nitridation process with Y₂O₃ addition. *Journal of the European Ceramic Society*, 38(4), pp.1170-1178.
- [39] Johnson K, Ström V, Wallenius J, Lopes D. Oxidation of accident tolerant fuel candidates. *Journal of Nuclear Science and Technology*. 2016;:1-7.

DEPARTMENT OF SOME SUBJECT OR TECHNOLOGY
CHALMERS UNIVERSITY OF TECHNOLOGY
Gothenburg, Sweden
www.chalmers.se



CHALMERS
UNIVERSITY OF TECHNOLOGY